

# Characterization of Surface-Modified Polyalkanoate Films for Biomedical Applications

Leoncio Garrido,<sup>1</sup> Ignacio Jiménez,<sup>2</sup> Gary Ellis,<sup>1</sup> Pilar Cano,<sup>1</sup> Jesús M. García-Martínez,<sup>1</sup> Laura López,<sup>3</sup> Enrique de la Peña<sup>3</sup>

<sup>1</sup>Instituto de Ciencia y Tecnología de Polímeros, CSIC, Juan de la Cierva 3, 28006 Madrid, Spain

<sup>2</sup>Instituto de Ciencia de Materiales de Madrid, CSIC, Sor Juana Inés de la Cruz 3, 28049 Madrid, Spain

<sup>3</sup>Fundación Hospital de Alcorcón, Avda. Villaviciosa 2, 28922 Alcorcón, Spain

Received 9 December 2009; accepted 6 June 2010

DOI 10.1002/app.32920

Published online 27 September 2010 in Wiley Online Library (wileyonlinelibrary.com).

**ABSTRACT:** Poly(3-hydroxybutyrate-co-3-hydroxyvalerate) (PHBHV) films prepared by solvent casting were treated with oxygen, argon, and nitrogen radiofrequency-generated plasmas. The analysis by attenuated total reflectance infrared spectroscopy and X-ray absorption near edge spectroscopy of modified surfaces showed an increase of hydroxyl and unsaturated groups, compared with unmodified surfaces. Water contact angles decreased after a short time of exposure (<30 s) for all types of plasma. At long exposure times (>30 s), the water contact angles appeared to be independent of treatment time for nitrogen and argon plasmas, whereas they continuously decreased for films treated with oxygen. HaCaT cultures

on nontreated and treated PHBHV films showed that short plasma exposures of 10–20 s improve cell attachment to a greater extent than long exposure times habitually used in polymer surface plasma treatment. The film surface topology did not influence cell attachment. These results illustrate the importance of a detailed characterization of the surface physicochemistry in plasma-modified substrates designed as part of a strategy to optimize specific cell–biomaterial interactions. © 2010 Wiley Periodicals, Inc. *J Appl Polym Sci* 119: 3286–3296, 2011

**Key words:** gas plasma; poly(3-hydroxybutyrate-co-3-hydroxyvalerate); modification; substrate; biodegradable

## INTRODUCTION

Promising approaches in cellular-based therapies for tissue engineering and regenerative medicine require adequate supports to host bioactive agents (e.g., cells, growth factors) and to prepare *in vitro* tissue replacements or to deliver these agents *in vivo* to the organ or tissue of interest.<sup>1–3</sup> Currently, the design and development of suitable supports for these applications are very active areas of research and, among different types of available materials, synthetic biocompatible and biodegradable polymers are considered a viable option.<sup>4</sup> In an ideal arrangement, substrates prepared with these polymers would provide a temporary support for cells while they synthesize their own extra-

cellular matrix and, when placed *in vivo*, they would offer the advantage of avoiding additional surgical procedures for their removal.<sup>5</sup> Furthermore, the preparation of bioactive substrates is possible by designing macromolecules for self-assembly<sup>6–8</sup> or by adding compounds and macromolecular fragments with functional groups that can provide specific cues to modulate cell behavior, e.g., adhesion, proliferation, differentiation.<sup>9,10</sup> For this purpose, physical (blending or mixing) and chemical (covalent bonding–grafting) methods may be used. Also, microfabrication and surface modification could be applied to control cell shape and function, and build custom-made substrates, satisfying the requirements for specific applications.<sup>11</sup>

Copolymers based on 3-hydroxybutyric and 3-hydroxyvaleric acids (see Fig. 1) are biocompatible and hydrolyze slowly in the human body, and they are used in the preparation of implants and scaffolds for tissue engineering and drug delivery.<sup>12–17</sup> Specifically, and for applications related to those described in this report, microperforated composites of poly(3-hydroxybutyrate-co-3-hydroxyvalerate) (PHBHV) with basal membrane matrices have been studied as a substrate for keratinocytes.<sup>18</sup> Also, thin films of poly(3-hydroxybutyrate) and PHBHV copolymers treated with different types of gas plasmas have been used as scaffolds for various cell types, i.e., fibroblasts, osteoblasts, and epithelial cells.<sup>19–25</sup>

Correspondence to: L. Garrido (garrido@ictp.csic.es).

Contract grant sponsor: the Ministerio de Ciencia e Innovación; contract grant number: CTQ2008-03229.

Contract grant sponsor: the Instituto de Salud Carlos III; contract grant numbers: FIS PI05/2087, PI05/1947.

Contract grant sponsor: Ministerio de Ciencia e Innovación (MICINN); contract grant number: MAT2009-13625.

Contract grant sponsor: the EU-FP6 “Research Infrastructure Action”; contract grant number: R II 3-CT-2004-506008.

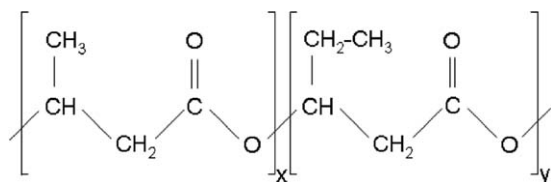


**Figure 1** Sketch illustrating the chemical structure of PHBHV.

Generally, fast cell attachment onto a substrate is sought to reduce apoptotic cell death,<sup>26</sup> and gas plasma treatment is often selected as a technique to modify the chemistry and wettability of polymer surfaces when used as cell substrates.<sup>27</sup> However, a wide range of experimental conditions used to specifically modify the surface of PHBHV films has been reported.<sup>19–25</sup> Specifically, treatment times that range between 10 s and 20 min, with comparable effective power, have been reported. Thus, an optimization of the procedure for the type of cells of interest in this study, keratinocytes, could be relevant. In this respect, it should be taken into consideration that the properties of plasma-modified surfaces mainly depend on parameters controlled by the reaction conditions (i.e., type of gas, pressure, radio-frequency, effective power, and time of treatment) and the properties of the polymer used.<sup>27</sup> Furthermore, the interaction between the modified surface and a particular cell would also be conditioned by cellular biological characteristics.<sup>28–31</sup> Therefore, a detailed knowledge of the physical and chemical properties of modified substrates is important to achieve a better understanding of cell–surface interactions and to design better substrates. In this regard, X-ray absorption near edge spectroscopy (XANES) has been shown to be a very useful technique for the characterization of the surface chemistry of polymer films.<sup>32,33</sup> This technique offers some advantages over the more common X-ray photoelectron spectroscopy (XPS). In particular, XANES provides unambiguous information regarding the formation of saturated or unsaturated bonds because the  $\pi$  and  $\sigma$  bands appear separated, unlike in XPS where the energy shift due to the type of hybridization is mixed with the true chemical shifts. Additionally, XANES peaks have an excitonic nature and, therefore, are narrower than the corresponding XPS peaks.

In this study, the preparation and characterization of flexible PHBHV films for cellular support, where gas plasma treatment was used to improve cell–biomaterial interactions, were described. The topology of the films was studied with atomic force microscopy (AFM), and the surface chemistry of films treated with oxygen, nitrogen, and argon plasmas was investigated with XANES and attenuated total

reflectance-infrared (ATR-IR) spectroscopy. In addition, cell attachment and morphology on nontreated and treated PHBHV substrates were illustrated.

## EXPERIMENTAL

### Preparation of PHBHV films

Poly(3-hydroxybutyrate-co-3-hydroxyvalerate) (PHBHV) with 11 mol % of hydroxyvalerate was purchased from Aldrich (Steinheim, Germany). Samples of PHBHV films were prepared by solvent casting from polymer solutions in chloroform (Carlo Erba Reactifs, SDS, val de Reuil Cedex, France) at a concentration of 36 g L<sup>-1</sup> into a glass mold. After casting, chloroform was slowly evaporated and the film was cut into 16-mm diameter disks of approximately 30- $\mu$ m thickness. These were stored in a desiccator under vacuum at room temperature until used.

### Surface modification by gas plasma treatment

Disks of PHBHV films for gas plasma treatment were placed in a home built cylindrical radio-frequency (RF) glow-discharge reactor. A quartz tube was used to house a RF coil with dimensions of 8 cm in diameter and 25 cm in length. After performing preliminary experiments to assess the optimum working pressure and RF power, the standard procedure of gas plasma treatment involved the evacuation of the chamber to 0.01 mbar, which was subsequently filled with oxygen, argon, or nitrogen gas to a working pressure of 0.1 mbar. At this point, the RF generator (operating at a frequency of 13.56 MHz) was activated at 100 W for 10–90 s. Samples were removed from the reactor within 10–15 min after finishing the plasma treatment. Some modified films were used within a week and others were stored under vacuum until used (up to 3 months, approximately).

### AFM

The surface topography analysis of PHBHV films was performed with a Multimode Veeco AFM with Nanoscope IV A controller (Veeco, Santa Barbara, CA) in tapping mode. Pyramidal phosphorous *n*-doped silicon cantilevers were used, as well as a resonance frequency of about 267 kHz. The manufacturer's software was used to determine the mean surface roughness.

### Surface characterization by XANES

The modified PHBHV films were characterized by XANES performed at Beamline PM4 with the SURICAT end station at the BESSY-II synchrotron (Berlin,

Germany). Data were acquired in total electron yield mode by recording the current drained to ground from the sample. The sample signal was normalized to the signal recorded simultaneously from a gold-covered grid located upstream in the X-ray path.

### Surface characterization by IR spectroscopy

ATR-IR spectroscopy was performed using a Seagull variable angle ATR (Harrick Scientific, New York) using a 25-mm diameter single reflection Ge crystal (refractive index,  $n = 4.0$ ). Spectra were recorded at incident angles between  $40^\circ$  and  $70^\circ$  using a Spectrum 2000 FTIR spectrometer (Perkin-Elmer, Beaconsfield, UK), at a spectral resolution of  $4\text{ cm}^{-1}$ , accumulating between 50 and 200 scans to improve data quality. All ATR spectra were corrected to absorbance spectra using a simple wavelength dependence rule by assuming optimum surface contact.

### Contact angle measurements

To determine alterations of the surface of PHBHV films caused by the gas plasma treatment, contact angles of deionized distilled water were measured for treated and nontreated surfaces using the sessile drop method with a Ramé-Hart goniometer (Netcong, NJ). The mean values reported were the results of at least eight measurements.

### Cell cultures

HaCaT cells are nontransformed, immortal human keratinocytes used as surrogates of interfollicular keratinocytes, and were a kind gift from N.E. Fusening (German Cancer Research Center, Heidelberg, Germany). These cells were genetically modified with retroviral vectors introducing the green fluorescence gene into the cell genome (EGFP), which conferred a green color to the epithelial cells facilitating their detection on the PHBHV surfaces.

The cell attachment experiments were performed on the PHBHV disks placed at the bottom of 24-well plates. All PHBHV films were rinsed briefly with a 70% ethanol solution and dried at room temperature immediately prior to use. A total of  $10^5$  HaCaT-EGFP (LV) cells were seeded onto the substrates and 2 mL of DMEM medium (Lonza, cat N°BE12-614F), supplemented with 10% fetal calf serum, was added carefully to avoid flotation of the PHBHV disks.

### Light microscopy: Cell attachment

Cell attachment performance was estimated by counting cells on the PHBHV substrates using an inverted light microscope (NIKON Eclipse T5100).

We considered that a flattened morphology was characteristic of an attached cell and that a rounded one corresponded to nonattached cells. Counting was performed at  $40\times$  magnification in five different fields of  $0.2\text{ mm}^2$ , 4 h after cell seeding.

PHBHV films treated with oxygen, nitrogen, and argon plasmas for periods of 10, 30, and 90 s were tested. The cell density was calculated using the data collected as described earlier.

### Scanning electron microscopy

Cultures were fixed with glutaraldehyde (1 : 100), then dehydrated stepwise with ethanol/water mixtures, with progressively increased concentrations of alcohol, and, finally, processed for electron microscopy. Scanning electron microscopy of gold-coated samples was performed on a Philips XL30 (Philips, Eindhoven, the Netherlands) microscope at ambient temperature by using the parameters indicated in each photograph.

### Mechanical properties measurements

Tensile mechanical properties were measured over small dog-bone samples, type 5B in the UNE-EN ISO 527-2 standard, with the exception of the sample thickness. The dog-bone samples were cut from PHBHV films in the contour dimensions required by means of a Frank Press. The parameters of the samples associated with the calculations were thickness ( $30\text{ }\mu\text{m}$ ), width (2.0 mm), and gauge length (20.0 mm). The samples were conditioned for 48 h at  $23^\circ\text{C}$  and 50% relative humidity, before performing measurements in an Instron 4200 dynamometer equipped with a 1 kN load cell at  $23^\circ\text{C}$  and 50% relative humidity. The crosshead speed was set at 1 mm/min. Calculations were performed by the instrumental software considering crosshead displacement. The following tensile parameters were obtained: modulus (nominal), tensile strength (nominal) and strain (nominal), the latter determined both at yield and at break point. In all cases, the results reported represent the average measurements of at least 10 samples.

### Statistical analysis

ANOVA was performed on contact angles and cell attachment data to estimate the variance at a significance level of 5% and statistical comparisons between treated and nontreated substrates were performed using two-tailed Student's  $t$  test. Statistical significance was considered for a  $P$  value of less than 0.05.

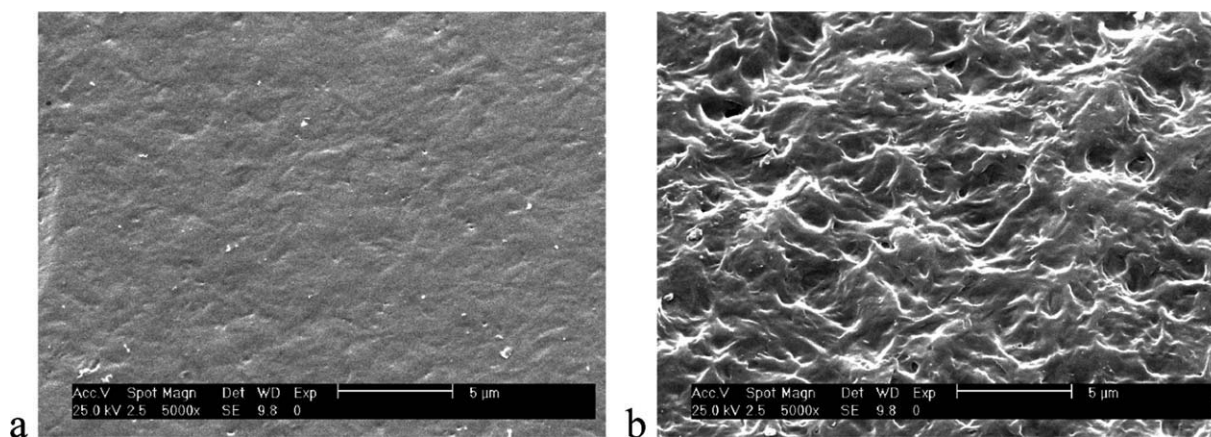


**Figure 2** Scanning electron micrographs of PHBHV film surfaces (a) in contact with glass and (b) exposed to air.

## RESULTS AND DISCUSSION

The importance of biomaterials chemistry and topography in cellular response and behavior is well recognized.<sup>34</sup> In our case, prior to studying the effect on cell cultures of surface modification of PHBHV films by plasma treatment, we investigated the influence of surface topography on cell attachment. The method used to prepare the PHBHV substrates, solvent casting into a glass mold, generated films with two types of surfaces, as illustrated in Figure 2. The side of the film in contact with the glass appeared smooth and glossy [Fig. 2(a)], whereas that in contact with air exhibited a rough and matte appearance [Fig. 2(b)]. The results of AFM measurements on glossy and matte surfaces provided mean roughness values of 22.3 and 109 nm, respectively. Nevertheless, the differences observed in the surface topography of nontreated substrates did not affect significantly ( $P = 0.32$ ) cell attachment, as illustrated in Figure 3, at least for the cell line used in this study.

Taking into account the results reported by Wang et al.<sup>23</sup> and after some preliminary measurements using various power settings, pressures and treatment times, the conditions indicated in the experimental section were selected. In all cases, the glossy side of the samples was used for surface modification and cell culture studies. It is relevant to highlight that the SEM analysis of PHBHV films did not reveal noticeable differences between the surface morphology of untreated and treated polymer substrates (see examples in Fig. 4). Pompe et al.<sup>24</sup> obtained similar results when comparing the topology of PHB films treated with plasma during 60–300 s with that of untreated films.

Samples of nontreated PHBHV films and those after a treatment of 60 s with nitrogen, oxygen, and argon gas plasmas were selected for analysis of the surface chemistry with XANES. The results are illustrated in Figure 5 and summarized in Table I. Figure 5(a)

shows the XANES survey spectra corresponding to samples of nontreated and gas plasma-treated PHBHV films, displaying the presence of C(1s), N(1s), and O(1s) core level transitions. The relative intensity of each transition is a metric of the atomic composition in the near surface ( $\sim 5$  nm) region. Note that the presence of nitrogen atoms is only detected for the plasma treatment with nitrogen gas. Figure 5(b) shows the XANES C(1s) spectra, normalized to the same height to evidence changes in the lineshape, corresponding to the aforementioned films and three reference samples. The latter were chosen as examples of C(1s) spectra for carbon atoms that have different types of covalent bonding. The graphite spectrum shows two main features, one at  $\sim 285.5$  eV, associated to the  $\pi^*$  resonance of C=C bonds ( $sp^2$ ), and the other at  $\sim 292.5$  eV, attributed to the  $\sigma^*$  resonance of C—C bonds ( $sp^3$ ). The C(1s) spectrum of diamond is shown as an example for  $sp^3$  hybrids. The polypropylene spectrum exhibits the corresponding  $\sigma^*$  resonances at  $\sim 287.5$  and 292 eV associated to the C—H and C—C bonds, respectively.<sup>35,36</sup>

The C(1s) XANES spectrum of nontreated PHBHV exhibits three main peaks: one at  $\sim 287.5$  eV,

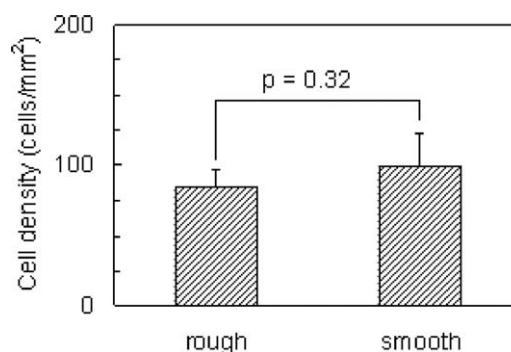


**Figure 3** Influence of PHBHV film topography on HaCaT attachment after 4 h of culture. No significant effect of surface roughness is observed ( $P = 0.32$ ).

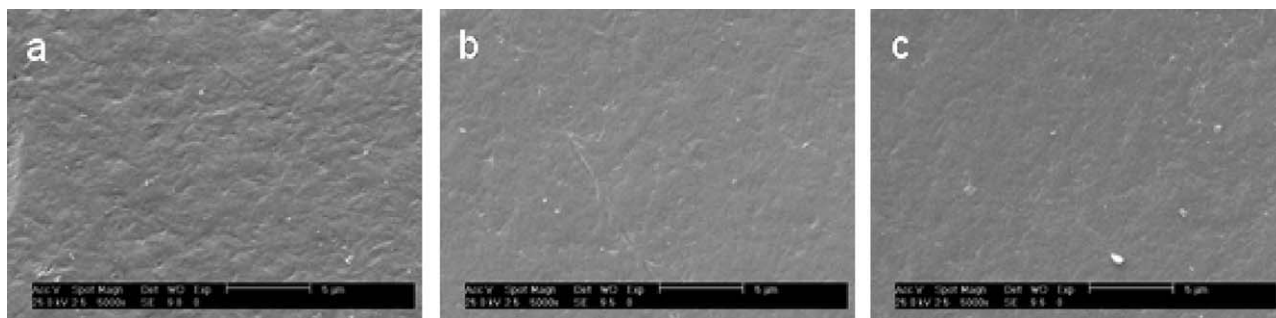


**Figure 4** Scanning electron micrographs of PHBHV film surfaces (a) nontreated, and treated during 60 s with gas plasma of (b) nitrogen and (c) oxygen.

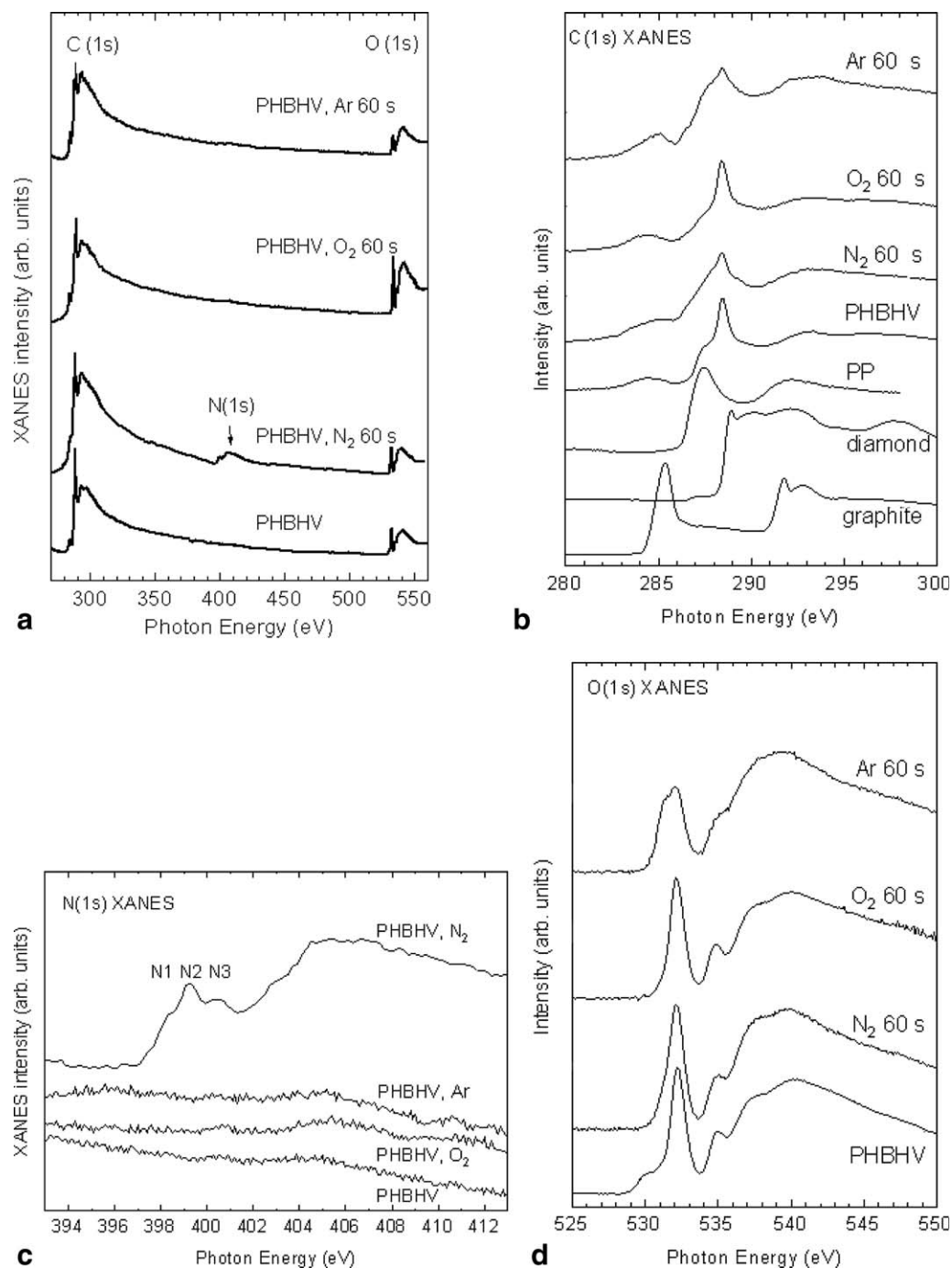


**Figure 5** XANES (a) survey, (b) C(1s), (c) N(1s), and (d) O(1s) spectra corresponding to nontreated and plasma-treated PHBHV films prepared by casting. (b) The C(1s) spectra of graphite, diamond, and polypropylene used as reference samples.

**TABLE I**  
**Signal Intensity Ratios Measured in XANES Spectra**  
**Corresponding to Samples of PHBHV Films Nontreated**  
**and Treated with Gas Plasma During 60 s**

Sample reference	Gas plasma	$I_N/I_C^a$	$I_O/I_C^b$
PHBHV N.T.	–	0	0.38
PHBHV N <sub>2</sub> , 60 s	Nitrogen	0.14	0.27
PHBHV O <sub>2</sub> , 60 s	Oxygen	0	0.67
PHBHV Ar, 60 s	Argon	0	0.33

<sup>a</sup> XANES nitrogen/carbon signal intensity ratio.

<sup>b</sup> XANES oxygen/carbon signal intensity ratio.

attributed to the  $\sigma^*$  resonance of C–H bonds not in the vicinity of oxygen containing functional groups; a second peak centered at  $\sim 288.5$  eV with contributions from the  $\pi^*$  resonance of C=O bonds and  $\sigma^*$  resonance of C–H bonds with the carbon atom bound also to oxygen; and a third peak at  $\sim 293$  eV with contributions from the  $\sigma^*$  resonance of C–C and C–O bonds.<sup>32,33</sup> The peak at 285 eV is characteristic of C=C  $\pi^*$  resonance and could be attributed to some beam damage to the polymer film.<sup>32</sup>

The profile of XANES spectra of treated films showed some variations compared with the spectra of nontreated films, depending on the type of gas used to generate the plasma. Thus, the spectra of films treated with nitrogen plasma show a decrease of carbonyl peak intensity and broadening of the C–H  $\sigma^*$  resonance due to contributions of newly formed C=N and C $\equiv$ N bonds with  $\pi^*$  resonances between  $\sim 286.5$  and  $\sim 287.5$  eV.<sup>32</sup> This is confirmed by the N(1s) XANES spectra shown in Figure 5(c). The incorporation of nitrogen to the film treated with nitrogen plasma is illustrated with the appearance of the peaks labeled N1, N2, and N3, corresponding to C=N, C $\equiv$ N, and (C–)<sub>3</sub>N  $\pi^*$  resonances, respectively.<sup>36</sup> In this figure, the N(1s) XANES spectra were not normalized to the same height, but displayed in absolute signal intensities, to show that functional groups with nitrogen in samples treated with argon and oxygen plasmas were not observed.

The C(1s) spectra of PHBHV films treated with oxygen showed a decrease in the C–H peak (287.5 eV) associated to the aliphatic carbons, most likely due to the incorporation of oxygen to the polymer with formation of C–O bonds (288.5 eV).<sup>37</sup> In fact, the treatment of PHBHV films with oxygen plasma increased the value of the XANES intensity ratio  $I_O/I_C$  from 0.38 to 0.67 (see Table I).

The films treated with argon plasma exhibited an increase in the intensity of the peak assigned to the C=C bonds. Also, a broadening of the peak associated to the carbonyl group (288.5 eV) was observed along with a decrease in its intensity. This broadening could be explained by an increase in the heterogeneity of the chemical environment of the carbonyl

groups, as shown in the corresponding XANES O(1s) spectrum discussed later. It should be noted that the presence of unsaturated carbon bonds was observed in all plasma-treated films, although it appeared to be greater in those treated with argon plasma.<sup>38</sup>

The results of XANES O(1s) spectra corresponding to PHBHV films are illustrated in Figure 5(d). The O(1s) spectrum of nontreated PHBHV exhibited three peaks at  $\sim 530$ ,  $\sim 532$ , and  $\sim 535$  eV associated to C=O  $\pi^*$  resonances, and several above at  $\sim 537$  eV attributed to the  $\sigma^*$  resonances of C–O and C=O bonds.<sup>37</sup> The treatment with gas plasma eliminated the peak at  $\sim 530$  eV in all spectra. The variations observed in the O(1s) spectra of the films treated with argon plasma were the most significant. The intensity of the peak at 532.2 eV was reduced whereas that of the peak at 531 eV increased. As the corresponding C(1s) spectrum showed earlier, treatment with argon increased the amount of unsaturated carbons,<sup>38</sup> and the presence of C=C groups near to C=O groups may have caused a partial shift in the  $\pi^*$  resonance of the carbonyls. The O(1s) spectra of saturated polyesters showed the highest carbonyl peak at 532 eV, while unsaturated polyesters demonstrated similar resonance at 531 eV.<sup>37</sup>

The observed values of the XANES intensity ratio  $I_O/I_C$  for all films are shown in Table I. As indicated earlier, only films treated with oxygen plasma exhibited an increase in the  $I_O/I_C$  compared with that in nontreated films. The ratio  $I_O/I_C$  was reduced in films treated with nitrogen plasma due to the incorporation of nitrogen to the polymer chains. The treatment with argon plasma reduced the ratio  $I_O/I_C$  due, most likely, to chain scission with formation of C=C bonds and CO<sub>2</sub>.<sup>38</sup>

The surface modification with plasma of PHBHV films alters their chemistry and, consequently, their wettability. Figure 6 illustrates the results of water contact angle measurements. A significant drop in the value of the contact angle occurred for those samples treated during only 10–20 s, changing from an initial value of  $72^\circ \pm 3^\circ$ , measured for the nontreated films, to  $\sim 55^\circ$  in the treated ones ( $P < 0.0001$ ). Further plasma exposure seemed to increase the wettability only in those films treated with oxygen ( $r^2 = 0.82$ ;  $P < 0.02$ ). These observations could be explained considering that the activation of a polymer surface by plasma occurs rapidly and effective modification could be achieved with residence times of less than 1 s.<sup>39</sup> Thus, the chemical functionalities produced initially increased the hydrophilicity of the film surface.

As the time of treatment increases, oxygen plasma generates oxygenated groups with hydrophilic character, whereas argon and nitrogen plasmas lead mainly to the formation of unsaturated C–C and

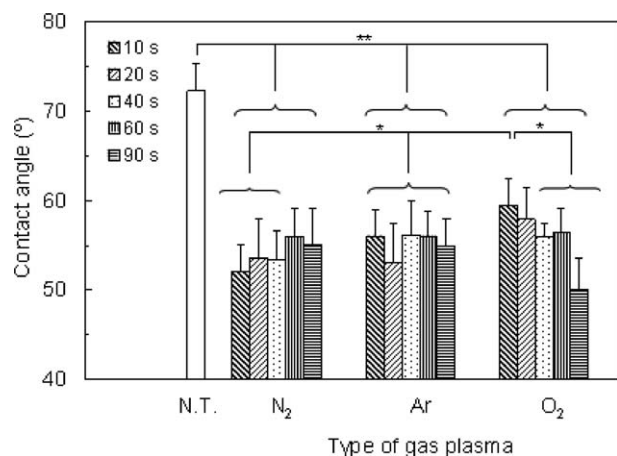


**Figure 6** Plot of water contact angle measurements as a function of time of treatment corresponding to nontreated (NT) and plasma-treated PHBHV films. Gas plasmas of oxygen (O<sub>2</sub>), argon (Ar), and nitrogen (N<sub>2</sub>) were used. *P* values at 95% confidence level are indicated by (\*\*) *P* < 0.0001 and (\*) *P* < 0.001.

C—N bonds, respectively, as shown earlier by XANES spectroscopy. An increase in these hydrophobic moieties appears to balance the hydrophilic functionalities that occur within the first minutes of exposure of treated samples to laboratory atmosphere.<sup>38</sup>

Physicochemical changes in plasma-modified surfaces of synthetic polymers after the initial treatment, i.e., aging, have been reported.<sup>38</sup> Generally, plasma-modified PHBHV samples were used within few days after the treatment. However, this did not occur always and, in some cases, samples were used up to 2 or 3 months after modification. Thus, water contact angles were measured at different times after plasma treatment to assess the aging of the modified PHBHV films. However, the results showed that the values of contact angles did not change significantly over a 3-month period, as illustrated in Table II.

Because water contact angle measurements demonstrated the most significant changes at short treatment times, we investigated the chemical changes on the surface of PHBHV films treated with plasma for 10 s using ATR-IR spectroscopy to assess whether the presence of hydrophilic groups could be detected. Variable angle ATR measurements using a Ge ATR crystal allowed us to characterize the surface of the samples at penetration depths <1 μm, significantly deeper than the XANES measurements. Because the depth of penetration,  $d_p$ , is a function of both the wavelength and the angle of incidence,  $\theta_i$ , of the IR radiation, for any given value  $\theta_i$  the high wavenumber region of the IR spectra is more surface-sensitive. For example, by varying the angle of incidence of the IR beam between 40° and 70°,  $d_p$  varies from 0.2 to 0.1 μm for the broad OH

stretching band centered at around 3255 cm<sup>-1</sup>, whereas for a band at 978 cm<sup>-1</sup>,  $d_p$  varies from 0.78 to 0.47 μm. Considering this, the IR spectra of untreated and treated PHBHV films were assessed.

A general observation was that treated films appeared to show an increase in hydroxyl groups with respect to the untreated films. As an example, the spectrum of a PHBHV film treated with argon for 10 s was compared with an untreated PHBHV film in Figure 7(a). Furthermore, in all the treated samples the carbonyl intensity also appeared to decrease, in agreement with the XANES data. As a measure of the effect of plasma treatment and time in the different samples, we have used the relative absorbance ratio of the integrated band areas of the broad OH stretching band centered at 3255 cm<sup>-1</sup> and the carbonyl stretching band at around 1720 cm<sup>-1</sup>. The value of this band area ratio is represented in Figure 7(b) as a function of the penetration depth considered at the frequency of the maximum  $\nu_{OH}$  band. It can be clearly observed that, at low penetration depths, a higher ratio is observed for treated samples, particularly in the case of nitrogen and argon plasma, and in the oxygen plasma with higher treatment time (data not shown). In addition, independently of the chemical changes that may have occurred in the polymer, the ATR results also show some slight differences in the crystallinity of the polymer that also vary with plasma treatment.

IR spectroscopy has been previously used to estimate the crystallinity in PHB and associated copolymers.<sup>40–42</sup> The relative intensity of a crystalline band at around 1228 cm<sup>-1</sup>, which corresponds to a vibrational mode associated with the helical chain conformation of the crystalline polymer,<sup>43</sup> is often used because it is absent in the spectra of amorphous material. The reference band relates to an asymmetric methylene deformation mode at around 1453 cm<sup>-1</sup>, reported to be independent of crystallinity.<sup>41</sup> In untreated PHBHV films, the crystallinity increased at greater distances from the surface. This was also observed in treated samples, however, the relative surface crystallinity estimated using the 1228/1453 cm<sup>-1</sup>

**TABLE II**  
Water Contact Angle Measurements of Aged Plasma-Modified PHBHV Substrates

Type of plasma	Time of treatment (s)	Contact angle <7 days after treatment	Contact angle 60–90 days after treatment
Oxygen	10	62 (2)	59 (2)
	60	56 (3)	56 (3)
Argon	10	56 (4)	56 (2)
	60	56 (3)	56 (3)
Nitrogen	10	50 (2)	52 (3)
	60	56 (4)	56 (3)

Values in parentheses represent standard deviation.

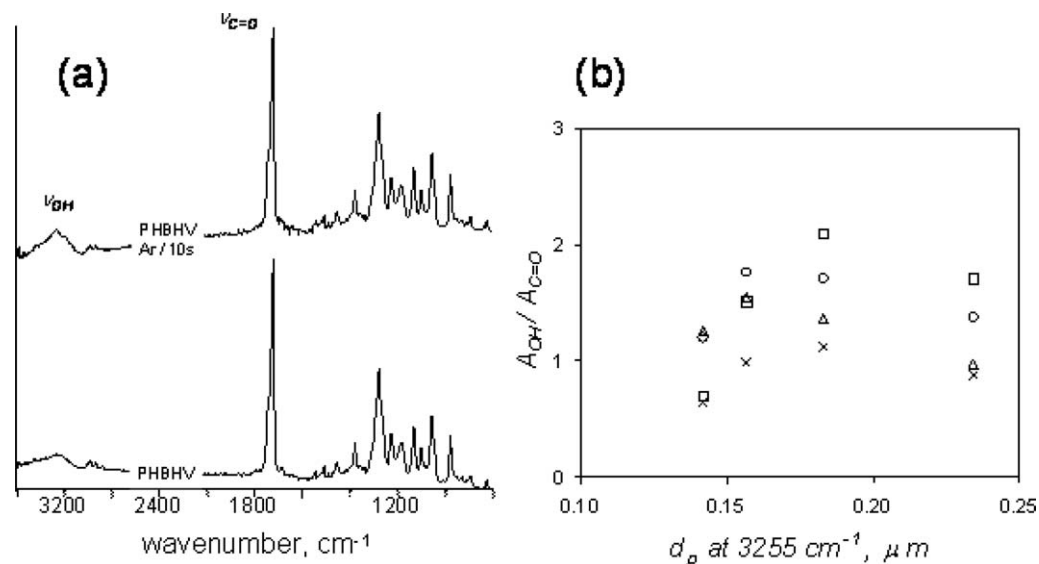


**Figure 7** (a) IR ATR spectra at an incident angle of 70° corresponding to untreated (bottom trace) and argon plasma treated during 10 s (top trace) PHBHV films (wavenumber scale change at 2000 cm<sup>-1</sup>), and (b) variations in hydroxyl band intensity relative to C=O band intensity as a function of penetration depth, *d<sub>p</sub>*, for different PHBHV film samples: ×, untreated, and treated with plasma of □, oxygen 10 s; ○, nitrogen 10 s; △, argon 10 s.

band ratio was clearly lower than that of untreated PHBHV in all cases, as demonstrated in Table III. This could facilitate the degradation of the modified substrates.

To determine the influence of plasma treatment on cell attachment to PHBHV films, samples subjected to short (10 s) and long (90 s) time exposures were selected. In addition, because the variation of water contact angles was not very large for films treated with the three types of plasma during 20–60 s, samples treated for an intermediate time of 30 s were chosen. The results are shown in Figure 8. The modification of PHBHV films improved the attachment of HaCaT cells to the polymer surfaces, particularly at short treatment times, independently of the type of gas used (*P* < 0.0001). Cell attachment to films treated with oxygen and argon was superior to that observed when using standard tissue culture polystyrene dishes. Longer exposure of PHBHV substrates to gas plasma did not seem to improve cell attachment. On the contrary, at 4 h after seeding, a decrease in cell density was observed with increas-

ing treatment time, particularly for those substrates treated with argon and oxygen plasmas (*P* < 0.02). These results suggest that, after the initial activation of the PHBHV surface which leads to a decrease of its hydrophobicity, the chemical functionality of the surface plays an important role.<sup>24,44,45</sup> It has been reported that water contact angles on polymer substrates of ~ 55° are optimal for cell adhesion.<sup>46</sup> However, the consideration of this factor alone does not seem to be sufficient to improve the interaction between substrate and cell, as shown here for films treated with argon and nitrogen plasmas. An increase in the presence of unsaturated bonds on the surface of substrates, as indicated by the XANES

**TABLE III**  
ATR-FTIR 1228/1453 cm<sup>-1</sup> Band Intensity Ratios Measured at Two IR Beam Incidence Angles, for Samples of Untreated and 10 s Plasma-Treated PHBHV Films

Type of plasma	Incidence angle, 70°	Incidence angle, 40°
NT	3.0	4.0
Argon	2.6	3.5
Nitrogen	2.2	3.1
Oxygen	2.7	4.1

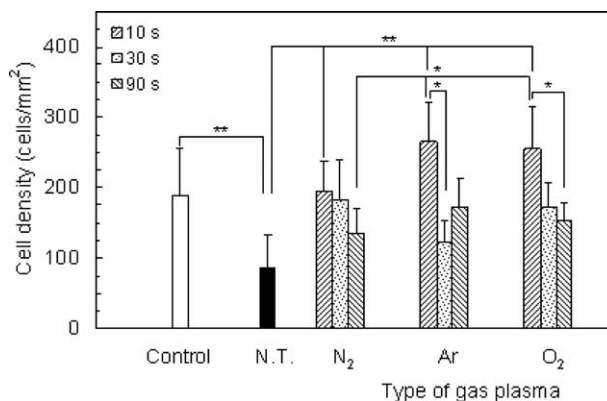


**Figure 8** HaCaT attachment on PHBHV films as a function of type of plasma used to modify the surface [oxygen (O<sub>2</sub>), argon (Ar), nitrogen (N<sub>2</sub>), nontreated (NT) and standard culture plate (control)] and time of exposure. *P* values at 95% confidence level are indicated by (\*\*) *P* < 0.0001 and (\*) *P* < 0.01.



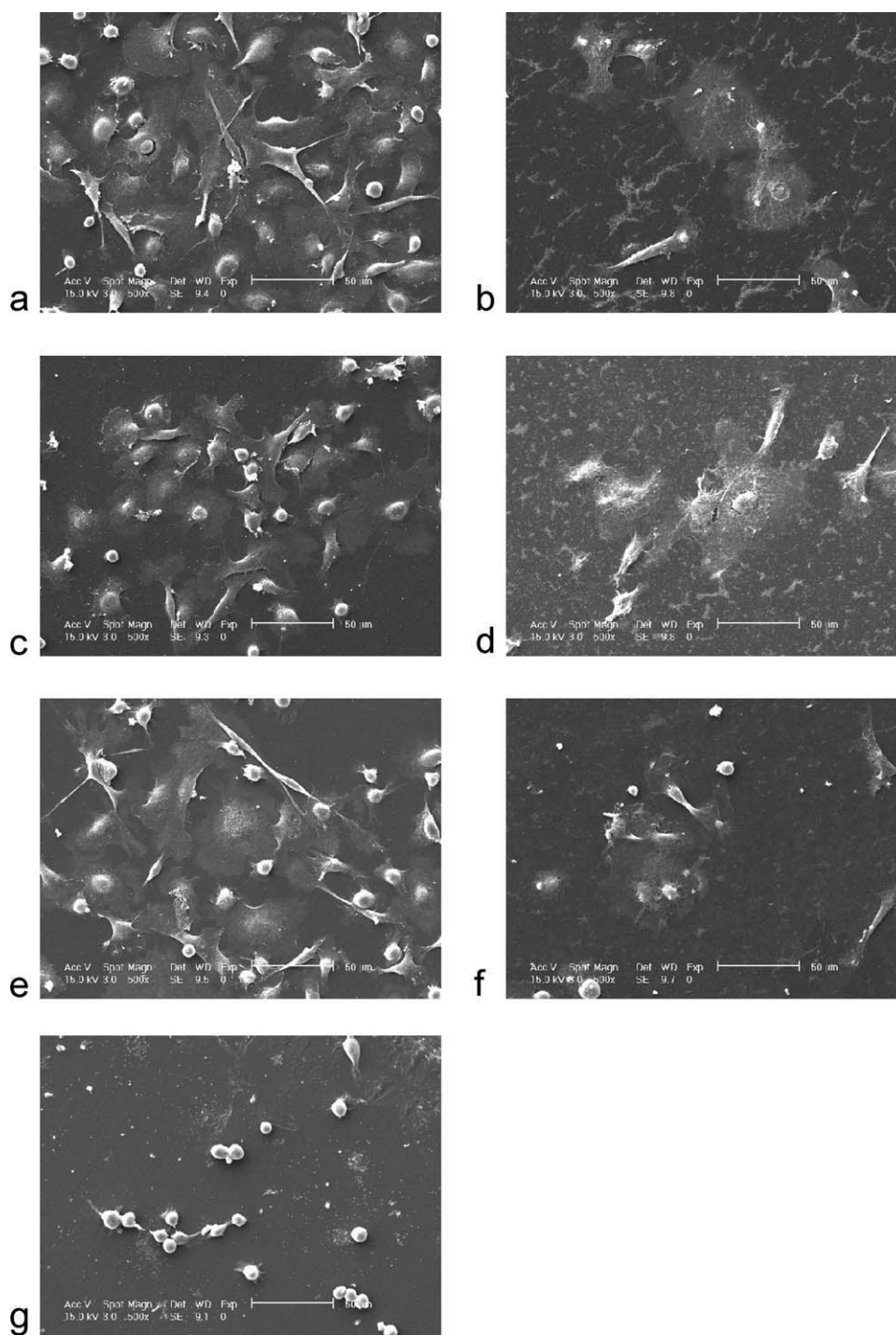


**Figure 9** Scanning electron micrographs illustrating the HaCaT cell morphology 4 h after cell seeding on PHBHV substrates modified with argon (a, b), nitrogen (c, d), and oxygen (e, f) plasmas during 10 and 90 s, respectively, and untreated (g).

results, may be responsible for the negative effect on cell adhesion.

Regarding treatments with oxygen, the wettability of the films increased with rising treatment times, although cell attachment decreased. This supports other reports suggesting that an increase in the presence of hydrophilic groups does not necessarily lead to an increase in cell adhesion.<sup>27,44</sup> Nevertheless, it

should be noted that all PHBHV films treated with oxygen plasma exhibited cell attachment equal or superior to standard tissue culture polystyrene.

Cell attachment findings were supported by SEM results illustrated in Figure 9. At short treatment times, all modified surfaces exhibited a high number of cells with a flattened appearance [Fig. 9(a,c,e)] compared to the untreated surfaces [Fig. 9(g)]. In the

**TABLE IV**  
**Tensile Parameters Determined in Samples of Untreated and 30 s O<sub>2</sub>**  
**Plasma-Treated PHBHV Films**

Sample reference	Module (MPa)	Strength at yield (MPa)	Strength at break (MPa)	Strain at yield (%)	Strain at break (%)
PHBHV	1050 ± 166	17.7 ± 5.4	17.7 ± 5.4	2.5 ± 1.0	2.5 ± 1.0
PHBHV O <sub>2</sub> , 30 s	1035 ± 133	22.2 ± 3.0	21.7 ± 3.1	3.6 ± 0.9	3.8 ± 1.0

case of films exposed to plasma for a longer time (90 s), a lower number of attached cells were observed [Fig. 9(b,d,f)]. In these films, an increase in the amount of deposits on the surfaces was also noted, probably arising from the cell culture medium.

Although we did not anticipate any significant influence of the plasma treatment upon the macroscopic properties of the films, their mechanical properties were studied in samples of PHBHV films untreated and treated with oxygen plasma for 30 s. The oxygen plasma treated sample was selected as a representative example, considering that cell attachment results do not support plasma exposures over 30 s. In addition, the cellular response to substrates treated with oxygen plasma was equal or better than the response to the other plasma treatments. Table IV summarizes the tensile parameters obtained. Almost all values for both the untreated and the plasma-treated specimens did not significantly differ and, therefore, the plasma treatment did not appreciably alter the mechanical properties of the polymer. Nevertheless, differences found between the values at break and those at yield point for treated samples suggest that there are at least some local changes in the polymer structure that induce the system to flow slightly after the yield point. This subtle change is in agreement with the ATR-FTIR results that showed a decrease in the crystallinity at the surface of the films after plasma treatment, which could lead to substrates exhibiting a less brittle behavior.

## CONCLUSIONS

PHBHV films were prepared by solvent casting, modified by treatment with gas plasma of oxygen, argon, and nitrogen, and tested as cell substrates. It was found that the topology of untreated films did not play a significant role on the attachment of keratinocytes to the substrate. The analysis of the surface chemistry of plasma-modified PHBHV films with IR and X-ray spectroscopies showed an increase in hydroxyl groups in all samples after short-time treatments. Long-time treatments lead to the formation of unsaturated carbons/hydrophobic species, particularly in films exposed to argon and nitrogen plasmas. In this regard, the use of XANES offered an advantage over XPS because it provided a better dis-

crimination between saturated and unsaturated carbon bonds. Although values of water contact angles for the treated surfaces were at, or near to, the reported optimal value to favor the cell–substrate interaction (about 55°) in all cases, the best results for the conditions used in this study were obtained with plasma exposure times of less than 30 s. The results from measurements of the mechanical properties suggest that no changes in the values of tensile parameters should be expected for <30 s exposure to the plasma. Finally, this study highlights the need for detailed characterization of the surface chemistry of polymer substrates to facilitate the development of optimal cell–substrate pairs. An important observation from a technological standpoint that results from this approach is the fact that effective plasma surface modification can be achieved with significantly shorter exposure times than those generally used.

The authors thank D. Gómez and M. Hernández of ICTP for technical assistance with SEM and AFM, respectively.

## References

1. Furth, M. E.; Atala, A.; van Dyke, M. E. *Biomaterials* 2007, 28, 5068.
2. Eisenbarth, E. *Adv Eng Mat* 2007, 9, 1051.
3. Buchmeiser, M. R. *J Polym Sci Part A: Polym Chem* 2009, 47, 2219.
4. Nair, L. S.; Laurencin, C. T. *Prog Polym Sci* 2007, 32, 762.
5. Causa, F.; Netti, P. A.; Ambrosio, L. A. *Biomaterials* 2007, 28, 5093.
6. Binder, W. H.; Sahsenhofer, R. *Macromol Rapid Commun* 2007, 28, 15.
7. Ariga, K.; Hill, J. P.; Lee, M. V.; Vinu, A.; Charvet, R.; Acharya, S. *Sci Technol Adv Mater* 2008, 9, 014109.
8. Nie, Z.; Kumacheva, E. *Nat Mater* 2008, 7, 277.
9. Anderson, D. G.; Burdick, J. A.; Langer, R. *Science* 2004, 305, 1923.
10. Lutolf, M. P.; Hubbell, J. A. *Nat Biotechnol* 2005, 23, 47.
11. Murphy, M. B.; Mikos, A. G. In *Principles of Tissue Engineering*, 3rd ed.; Lanza, R., Langer, R., Vacanti, J., Eds.; Academic Press: New York, 2007; pp. 309–321.
12. Holl, S. J.; Jolly, A. M.; Yasin, M.; Tighe, B. *J Biomaterials* 1987, 8, 289.
13. Holl, S. J.; Yasin, M.; Tighe, B. *J Biomaterials* 1990, 11, 206.
14. Saito, T.; Tomita, K.; Juni, K.; Ooba, K. *Biomaterials* 1991, 12, 309.
15. Gogolewsky, S.; Jovanovic, M.; Perren, S. M.; Dillon, J. G.; Hughes, M. K. *J Biomed Mat Res* 1993, 27, 1135.
16. Freier, T. *Adv Polym Sci* 2006, 203, 1.

17. Williams, S. F.; Martin, D. P.; Horowitz, D. M.; Peoples, O. P. *Int J Biol Macromol* 1999, 25, 111.
18. Serrano, F.; Lopez, L.; Jadraque, M.; Koper, M.; Ellis, G.; Cano, P.; Martin, M.; Garrido, L. *Biomaterials* 2007, 28, 650.
19. Kang, I. K.; Choi, S. H.; Shin, D. S.; Yoon, S. C. *Int J Biol Macromol* 2001, 28, 205.
20. Hasirci, V.; Tezcaner, A.; Hasirci, N.; Süzer, Ş. *J Appl Polym Sci* 2003, 87, 1285.
21. Tezcaner, A.; Bugra, K.; Hasirci, V. *Biomaterials* 2003, 24, 4573.
22. Köse, G. T.; Korkusuz, F.; Korkusuz, P.; Purali, N.; Özkule, A.; Hasirci, V. *Biomaterials* 2003, 24, 4999.
23. Wang, Y.; Lu, L.; Zheng, Y.; Chen, X. *J Biomed Mater Res* 2006, 76A, 589.
24. Pompe, T.; Keller, K.; Mothes, G.; Nitschke, M.; Teese, M.; Zimmermann, R.; Werner, C. *Biomaterials* 2007, 28, 28.
25. Lucchesi, C.; Ferreira, B. M. P.; Duek, E. A. R.; Santos, A. R.; Jr. Joazeiro, P. P. *J Mater Sci Mater Med* 2008, 19, 635.
26. Banes, A. J.; Wall, M.; Gravin, J.; Archmbault, J. In *Functional Tissue Engineering*; Guilak, F., Butler, D. L., Goldstein, S. A., Mooney, D. J., Eds.; Springer-Verlag, New York, 2003; pp 318–334.
27. Siow, K. S.; Britcher, L.; Kumar, S.; Griesser, H. J. *Plasma Process Polym* 2006, 3, 392.
28. De Bartolo, L.; Morelli, S.; Bader, A.; Drioli, E. *J Mater Sci Mater Med* 2001, 12, 959.
29. Satriano, C.; Carnazza, S.; Guglielmino, S.; Marletta, G. *Nucl Instrum Meth B* 2003, 208, 287.
30. Ozcan, C.; Hasirci, N. *J Biomat Sci Polym Ed* 2007, 18, 759.
31. Ozcan, C.; Zorlutuna, P.; Hasirci, V.; Hasirci, N. *Macromol Symp* 2008, 269, 128.
32. Kikuma, J.; Tonner, B. P. *J Electron Spectrosc Relat Phenom* 1996, 82, 53.
33. Dhez, O.; Ade, H.; Urquhart, S. G. *J Electron Spectrosc Relat Phenom* 2003, 128, 85.
34. Saltzman, W. M.; Kyriakides, T. R. In *Principles of Tissue Engineering*, 3rd ed.; Lanza, R., Langer, R., Vacanti, J., Eds.; Academic Press: New York, 2007; pp 279–296.
35. Ade, H.; Urquhart, S. G. In *Chemical Application of Synchrotron Radiation*; Sham, T. K., Ed.; World Scientific Publishing: River Edge, NJ, 2002; pp 285–355.
36. Alonso, F.; Gago, R.; Jiménez, I.; Gómez-Aleixre, C.; Kreissig, U.; Albella, J. M. *Diamond Relat Mater* 2002, 11, 1161.
37. Urquhart, S. G.; Ade, H. *J Phys Chem B* 2002, 106, 8531.
38. France, R. M.; Short, R. D. *J Chem Soc Faraday Trans* 1997, 93, 3173.
39. Förch, R.; Zhang, Z.; Knoll, W. *Plasma Process Polym* 2005, 2, 351.
40. Galego, N.; Rozsa, C.; Sanchez, R.; Fung, J.; Vazquez, A.; Tomás, J. S. *Polym Test* 2000, 19, 485.
41. Xu, J.; Guo, B. H.; Yang, R.; Wu, Q.; Chen, G. Q.; Zhang, Z. M. *Polymer* 2002, 43, 6893.
42. Hong, S. G.; Chen, W. M. *e-Polymers* 2006, 1024, 1.
43. Wu, Q.; Tian, G.; Sun, S. Q.; Noda, I.; Chen, G. Q. *J Appl Polym Sci* 2001, 82, 934.
44. Lee, J. H.; Jung, H. W.; Kang, I.-K.; Lee, H. B. *Biomaterials* 1994, 15, 705.
45. Curran, J. M.; Chen, R.; Hunt, J. A. *Biomaterials* 2006, 27, 4783.
46. Lee, J. H.; Khang, G.; Lee, J. W.; Lee, H. B. *J Colloid Interface Sci* 1998, 205, 323.